

Supplementary Information for

## Hydrophobic immiscibility controls self-sorting or co-assembly of peptide amphiphiles

Rie Wakabayashi,<sup>\*,a</sup> Rino Imatani,<sup>a</sup> Mutsuhiro Katsuya,<sup>a</sup> Yuji Higuchi,<sup>b</sup> Hiroshi Noguchi,<sup>b</sup> Noriho Kamiya,<sup>a,c</sup> and Masahiro Goto<sup>a,c</sup>

[a] *Department of Applied Chemistry, Graduate School of Engineering, Kyushu University, 744 Motoooka, Nishi-ku, Fukuoka 819-0395, Japan.*

[b] *Institute for Solid State Physics, The University of Tokyo, Kashiwanoha 5-1-5, Kashiwa, Chiba 277-8581, Japan.*

[c] *Center for Future Chemistry, Kyushu University, 744 Motoooka, Nishi-ku, Fukuoka 819-0395, Japan.*

\*Corresponding author.

E-mail: wakabayashi.rie.122@m.kyushu-u.ac.jp

### Table of Contents

1. Materials and methods	S1
2. Synthesis of PAs	S3
3. CLSM images of H-PA and F-PA assemblies	S4
4. Time-dependent FT-IR, fluorescent, and dynamic light scattering measurement	S5
5. Synthesis of fluorescence probe-attached PAs	S8
6. Selective staining of H-PA and F-PA assemblies using fluorescence probe-attached PAs	S9
7. Self-sorting behaviour of H-PA/F-PA assemblies	S10
8. Co-assembly formation of H-PA-2/F-PA-2 upon incubation at high temperature	S11
9. Fluorescence resonance energy transfer analysis of H-PA-2/F-PA-2 assemblies	S11
10. Assembly formation with and without incubation at 363 K	S13
11. Dissipative particle dynamics simulation	S15

## 1. Materials and methods

### Materials.

*O*-(benzotriazol-1-yl)-*N,N,N',N'*-tetramethyluronium hexafluorophosphate (HBTU), 1-hydroxy-1H-benzotriazole monohydrate (HOBt), diisopropylethylamine (DIEA), 20% piperidine in DMF, trifluoroacetic acid (TFA), Fmoc-Glu(OtBu)-Alko Resin, Fmoc-Glu(OtBu)-OH · H<sub>2</sub>O, Fmoc-Gly-OH, Fmoc-Tyr(tBu)-OH, Fmoc-Phe-OH, Fmoc-Lys(Fmoc)-OH, Fmoc-Lys(Mmt)-Alko PEG Resin were obtained from Watanabe Chemical Industries (Hiroshima, Japan). Decanoic acid (C<sub>10</sub>), 2H,2H,3H,3H-heptadecafluoroundecanoic acid (HFU), and Fmoc-pentafluoro-L-phenylalanine were purchased from Tokyo Chemical Industry (Tokyo, Japan). 4,4,5,5,6,6,7,7,8,8,9,9,9-Tridecafluorononanoic acid (TFN) and thioflavin T (ThT) were from Sigma Aldrich (St. Louis, MO, USA). NHS-Fluorescein and 5-(and-6)-carboxytetramethylrhodamine succinimidyl ester were obtained from Thermo Fisher Scientific (Waltham, MA, USA). Methanol, *N,N*-dimethylformamide (DMF), and calcium chloride were obtained from Kishida Chemical (Osaka, Japan). Lauric acid (C<sub>12</sub>), triisopropylsilane, dichloromethane, diethyl ether, acetonitrile (ACN), and ammonia solution were obtained from FUJIFILM Wako Pure Chemical (Osaka, Japan). Reagents for Kaiser Test was purchased from Kokusan Chemical (Tokyo, Japan). 2-Morpholinoethanesulfonic acid (MES) was purchased from DOJINDO (Kumamoto, Japan).

### Methods.

MALDI TOF MS was measured with Auto flex-III (Bruker, Billerica, MA, USA) using  $\alpha$ -cyano-4-hydroxycinnamic acid (CHCA) as the matrix. Fluorescence spectra were recorded on a LS55 (PerkinElmer, Waltham, MA, USA). Fourier-transform infrared (FT-IR) spectra were recorded on a Spectrum Two (PerkinElmer). PA assemblies in 25 mM MES buffer (pH 7.0) were freeze-dried and spectra were obtained using ATR mode. Dynamic light scattering (DLS) measurements were conducted using a Nano-ZSP (Malvern Panalytical, Worcestershire, UK). Morphological observation was conducted by transmission electron microscopy (TEM) using a JEM-2010 (JEOL, Tokyo, Japan). Assemblies were drop-cast onto a STEM grid with an elastic carbon film (Okenshoji, Tokyo, Japan), stained with 2% uranyl acetate, dried in vacuo, and imaged at an accelerating voltage of 120 kV. Confocal fluorescence images were taken using an LSM700 microscope (Carl Zeiss, Oberkochen, Germany) with diode lasers (405 nm for ThT, 488 nm for FL, 555 nm for TMR). Emission filter/variable secondary dichroic beamsplitter used were None/478, BP 490-555/556, and None/559 for ThT, FL, and TMR, respectively. PA assemblies in 25 mM MES buffer (pH 7.0) were diluted 10- to 50-fold using the buffer,

cast on a multi-well glass-bottom dish (Matsunami, Osaka, Japan), and added with 10 mM CaCl<sub>2</sub> for the observation.

## 2. Synthesis of PAs

A standard *N*- $\alpha$ -9-fluorenylmethoxycarbonyl (Fmoc) solid-phase peptide synthesis method was applied for the synthesis of H-PAs and F-PAs using the Fmoc-Glu(OtBu)-Alko resin. For the coupling cycle of each amino acid, a mixture of coupling reagents (Fmoc-amino acid:HBTU:HOBt:DIEA = 3:3:3:6 mol equivalent to reactive sites on resin) in DMF was added and the reaction was conducted for 1 h at r.t. After each coupling reaction, Fmoc group was removed by the reaction with 20% piperidine in DMF for 10 min at r.t. After all amino acids were coupled, hydrophobic tails were attached using 10 equivalent of acids for C<sub>10</sub> and C<sub>12</sub> or 4 equivalent for HFU and TFN.

PA was cleaved from the resin by treating with the mixture of TFA: triisopropylsilane:water = 95:2.5:2.5 (vol:vol:vol) for 1.5 h. After the removal of the solvents under reduced pressure, PAs were precipitated and washed with cold diethyl ether. The crude solids were collected and purified by HPLC on InertSustain C18 column (GL science, Tokyo, Japan) using a gradient of water and ACN both containing 0.1% ammonia solution. The fractions with products were collected and lyophilized, and stored at -20°C. The obtained PAs were analyzed by HPLC (InertSustain C18 column, GL science) and MALDI TOF MS using CHCA as the matrix.

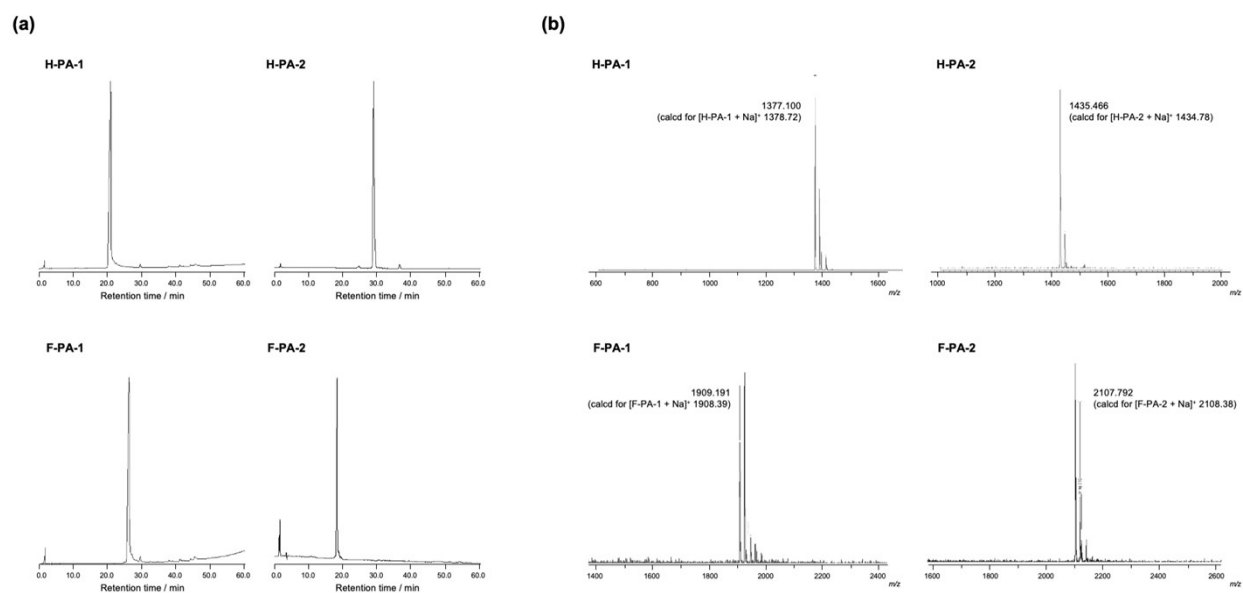


**Fig. S1** Characterization of H-PAs and F-PAs by HPLC (a) and MALDI TOF MS (b). Conditions: (a) InertSustain C18 (GL science, 4.6mm 250 mm), 10%B to 50%B in 60 min (H-PA1 and F-PA-1) or 20%B to 60%B in 60 min (H-PA2 and F-PA-2) (A: water, B: acetonitrile containing 0.1% ammonia solution), 1 mL/min, 220 nm detection. (b) Reflector positive mode using  $\alpha$ -CHCA as the matrix.

### 3. CLSM images of H-PA and F-PA assemblies

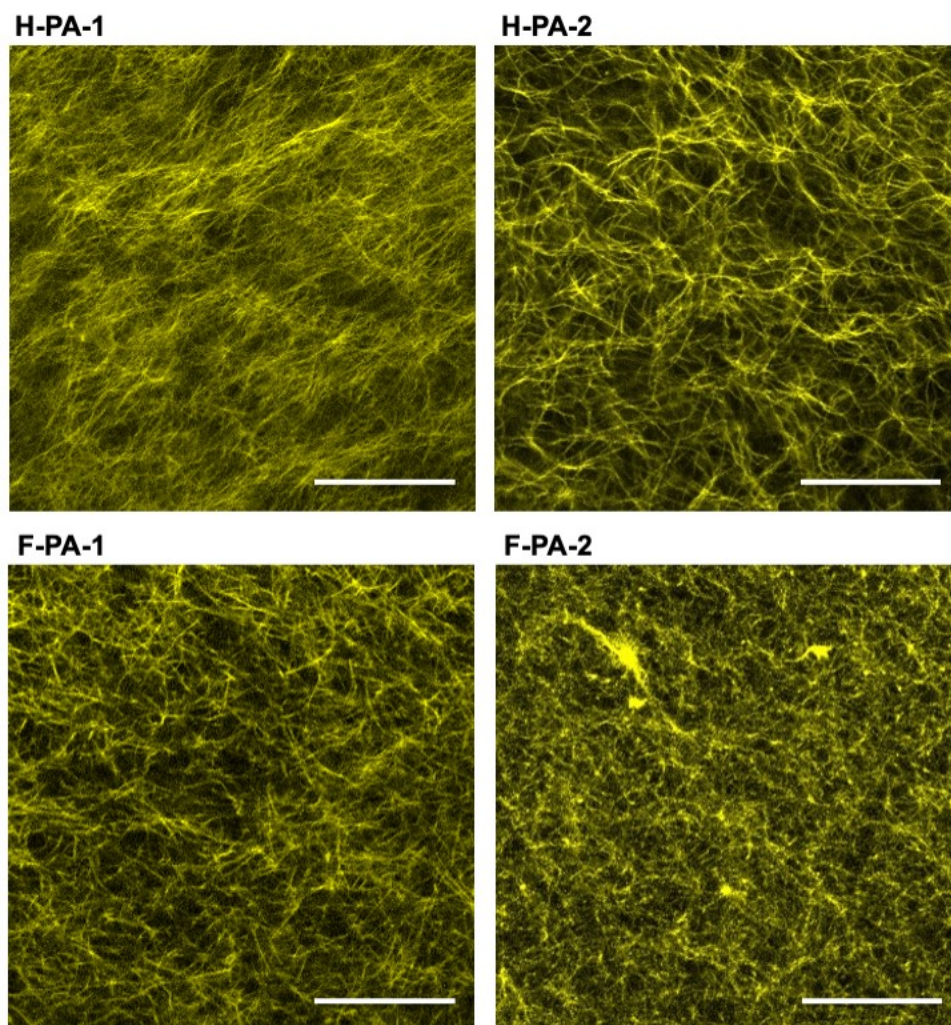


**Fig. S2** CLSM images of H-PA and F-PA assemblies ( $[PA] = 0.5$  mM in 25 mM MES (pH 7.0)). Thioflavin T was used to stain PA assemblies. Bars: 20  $\mu$ M.

#### 4. Time-dependent FT-IR, fluorescent, and dynamic light scattering measurement

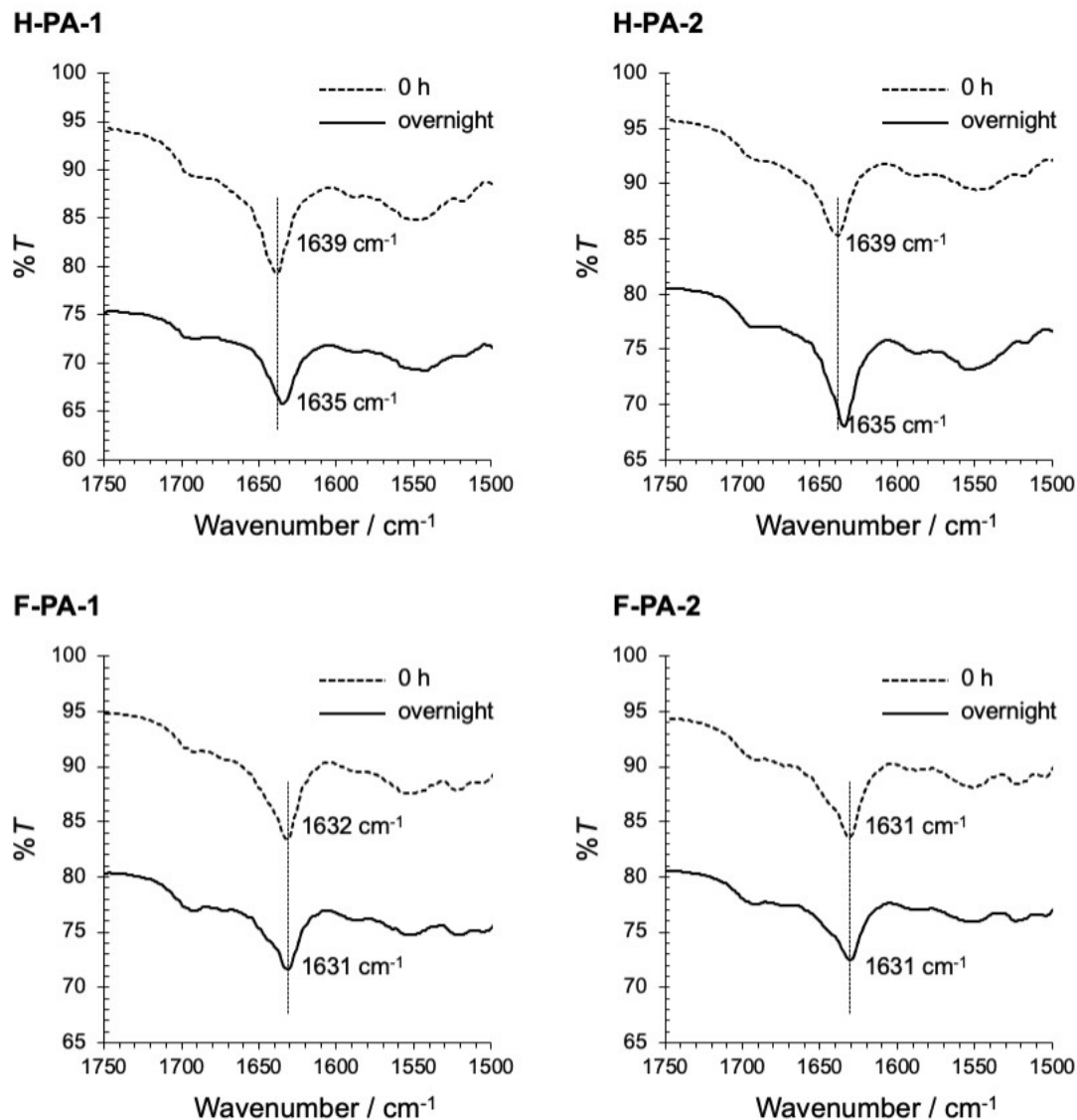


**Fig. S3** Time-dependent FT-IR measurement of H-PA and F-PA assemblies. PA solids were dispersed in 25 mM MES buffer (pH 7.0) at concentrations of 0.5 mM, heated using a heat-gun, cooled from 363 to 310 K by 3 K/min. PA dispersions were taken immediately after the solution reached 310 K (0 h) or after incubated overnight (overnight), freeze-dried, and spectra were obtained using ATR mode.

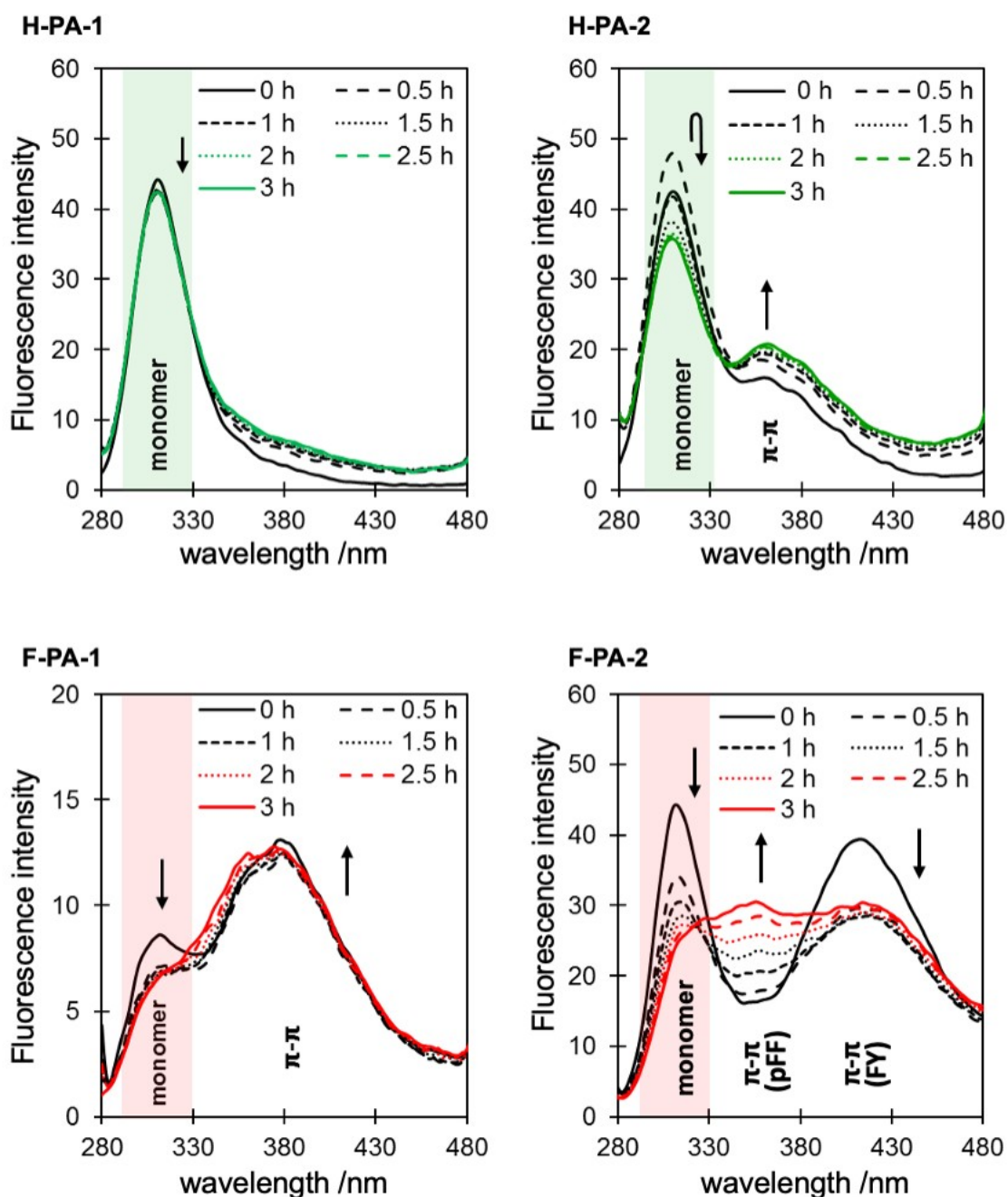


**Fig. S4** Time-dependent fluorescence spectral measurement of H-PA and F-PA assemblies. PA solids were dispersed in 25 mM MES buffer (pH 7.0) at concentrations of 0.5 mM, heated using a heat-gun, cooled from 363 to 310 K by 3 K/min. Fluorescence spectral measurement was started immediately after the solution reached 310 K.  $\lambda_{\text{ex}} = 260$  nm,  $T = 310$  K.

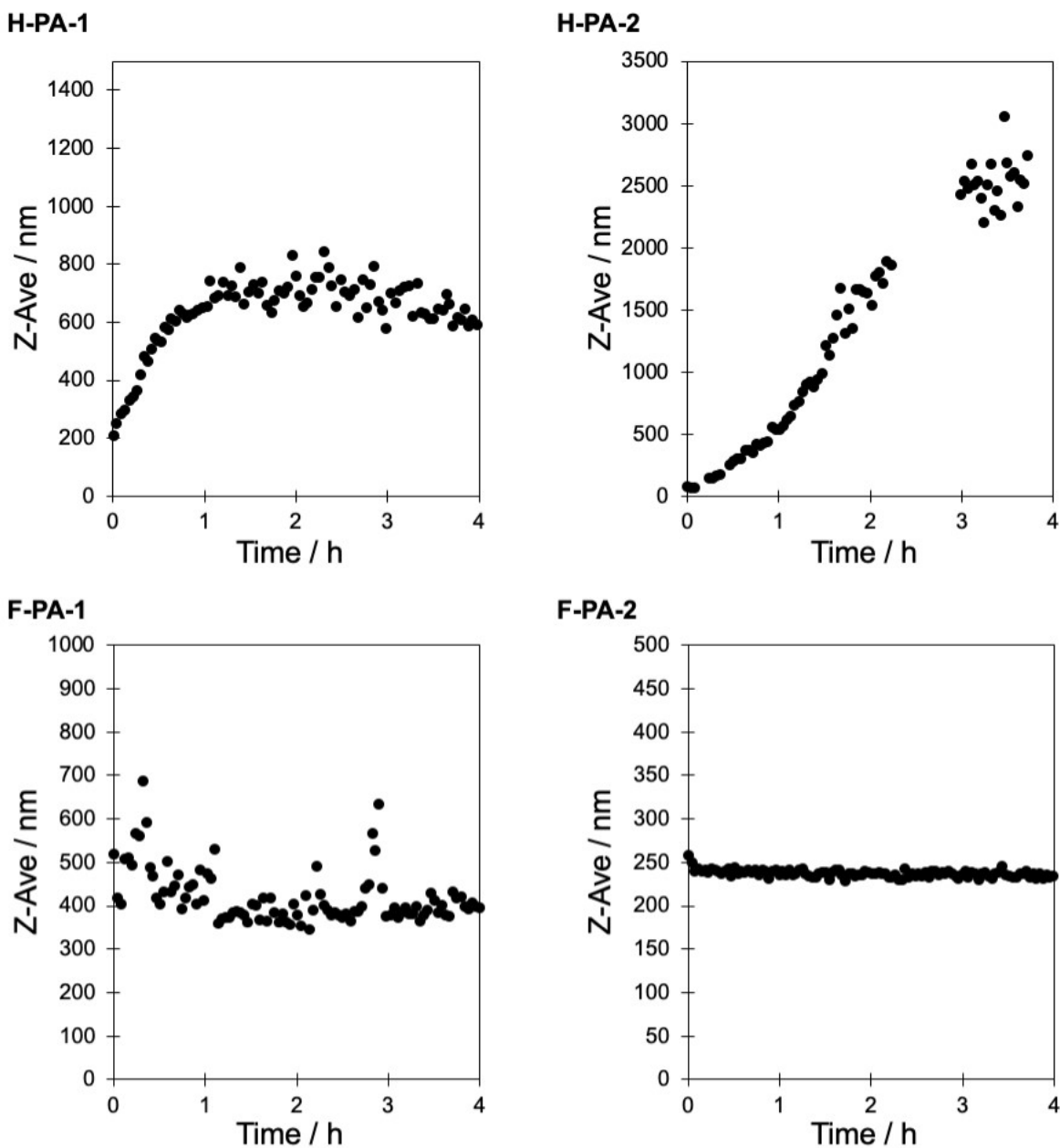


**Fig. S5** Time-dependent DLS measurement of H-PA and F-PA assemblies. PA solids were dispersed in 25 mM MES buffer (pH 7.0) at concentrations of 0.5 mM, heated using a heat-gun, cooled from 363 to 310 K by 3 K/min. DLS measurement was started immediately after the solution reached 310 K. T = 310 K.



## 5. Synthesis of fluorescence probe-attached PAs

Fluorescence probe fluorescein (FL) or tetramethylrhodamine (TMR)-attached PAs were synthesized using a standard Fmoc solid-phase peptide synthesis method in the same procedure as H-PAs and F-PAs. Fmoc-Lys(Mmt)-Alko resin was used for the synthesis. After all amino acids and hydrophobic tails were coupled, the protective Mmt group was removed by treating the resin with 1 % TFA in DCM, and NHS ester of fluorescence probe was reacted at r.t. overnight. The cleavage from the resin, purification, and analysis of PAs were done in the same procedure as H-PAs and F-PAs.

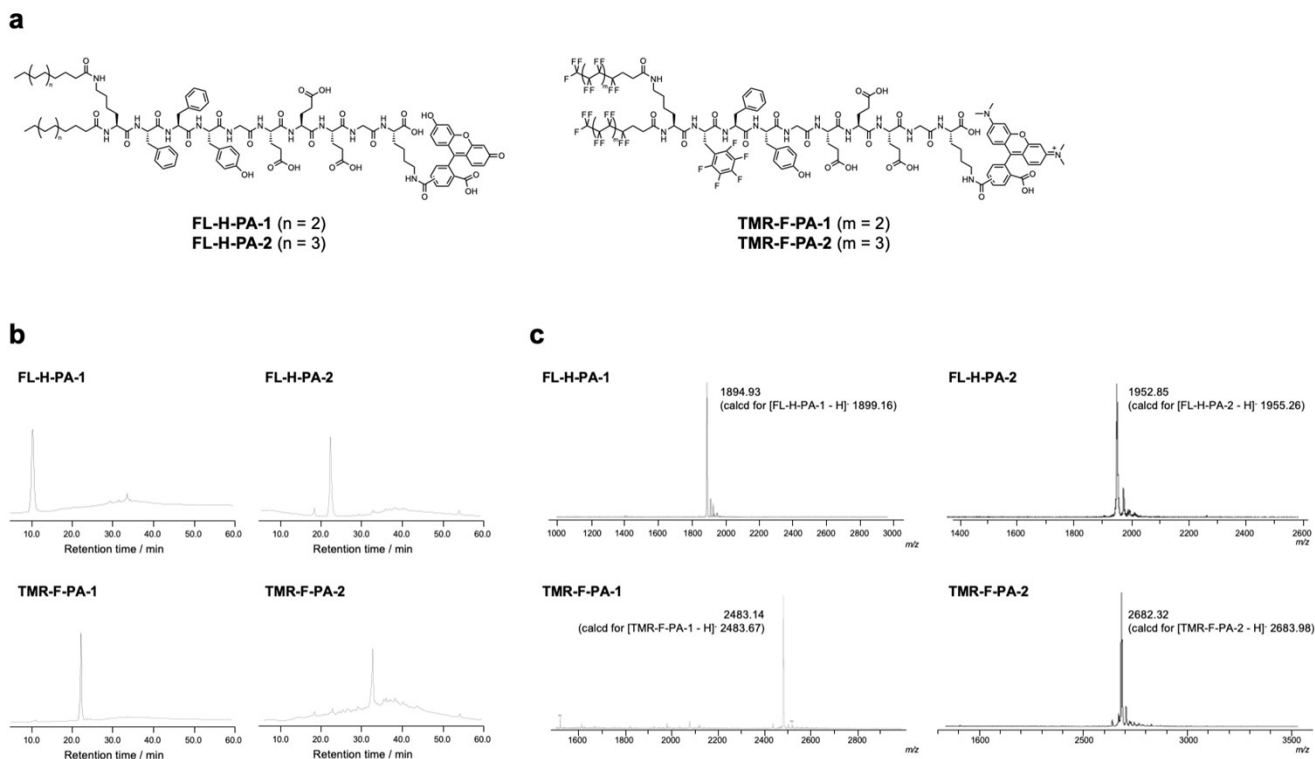


**Fig. S6** Chemical structures (a) and characterization of H-PAs and F-PAs by HPLC (b) and MALDI TOF MS (c). Conditions: (b) InertSustain C18 (GL science, 4.6mm 250 mm), 10%B to 100%B in 90 min (FL-H-PA1 and TMR-F-PA-1) or 5%B to 80%B in 75 min (FL-H-PA2 and TMR-F-PA-2) (A: water, B: acetonitrile containing 0.1% ammonia solution), 1 mL/min, 220 nm detection. (c) Linear negative mode using  $\alpha$ -CHCA as the matrix.

## 6. Selective staining of H-PA and F-PA assemblies using fluorescence probe-attached PAs

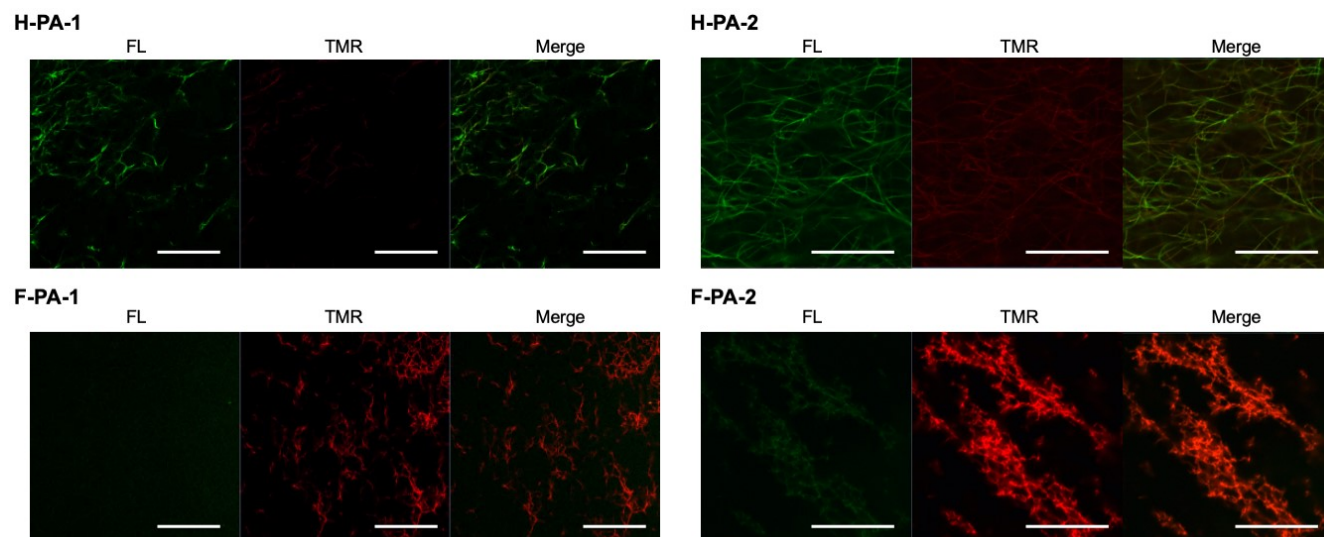


**Fig. S7** Confocal microscopy images of H-PAs and F-PAs (0.5 mM in 25 mM MES buffer, pH 7.0) in the presence of 1 mol% FL-H-PAs and TMR-F-PAs. Bars: 20  $\mu$ m.

## 7. Self-sorting behaviour of H-PA/F-PA assemblies

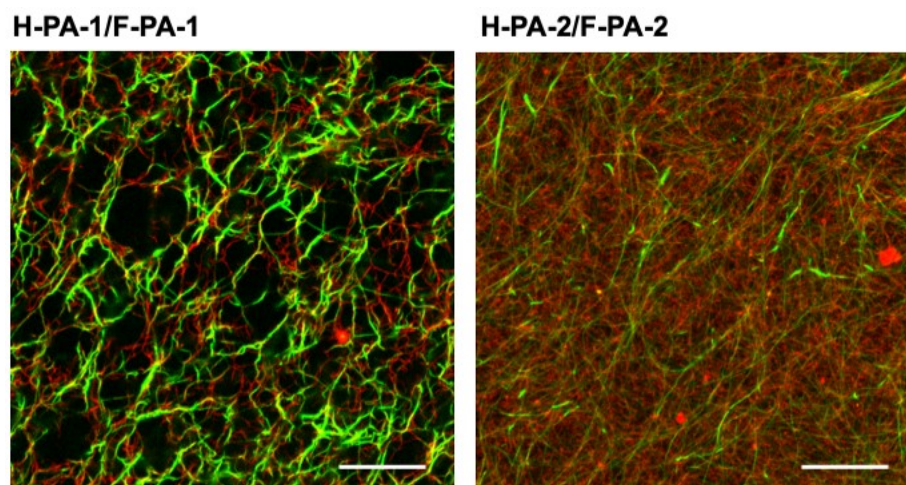


**Fig. S8** Projection of a stack of confocal microscopy images of H-PA-1/F-PA-1 and H-PA-2/F-PA-2 (H-PA:F-PA = 1:1 (mol/mol),  $[PA_{total}] = 0.5$  mM in 25 mM MES buffer, pH 7.0) in the presence of 1 mol% FL-H-PAs and TMR-F-PAs. Bars: 20  $\mu$ m.

## 8. Co-assembly formation of H-PA-2/F-PA-2 upon incubation at high temperature

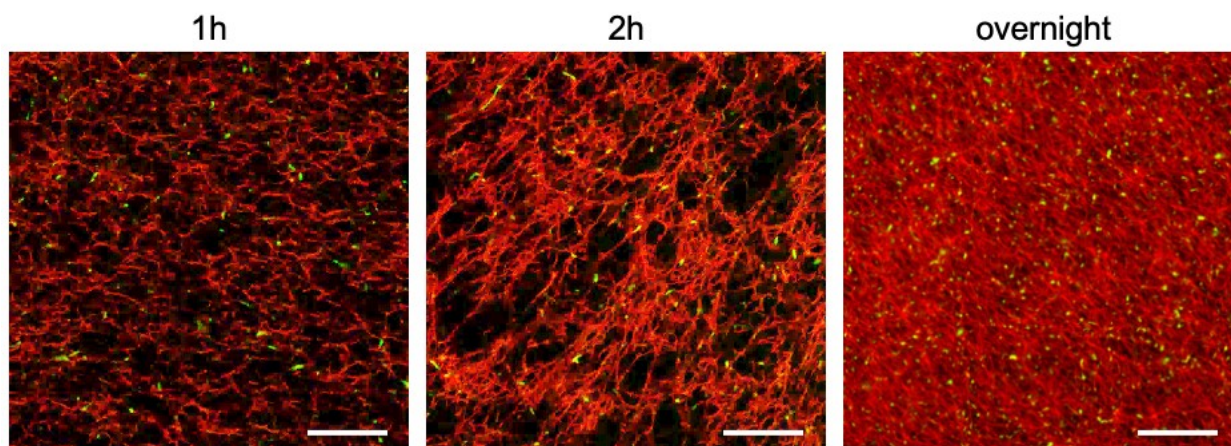


**Fig. S9** Confocal microscopy images of H-PA-2/F-PA-2 mixture (H-PA-2:F-PA-2 = 1:1 (mol/mol),  $[PA_{total}] = 0.5$  mM in 25 mM MES buffer, pH 7.0) in the presence of 1 mol% FL-H-PA-2 and TMR-F-PA-2. PA mixture was incubated at 363 K for 1h, 2h or overnight before cooling to 310 K. Bars: 20  $\mu$ m.

## 9. Fluorescence resonance energy transfer analysis of H-PA-2/F-PA-2 assemblies

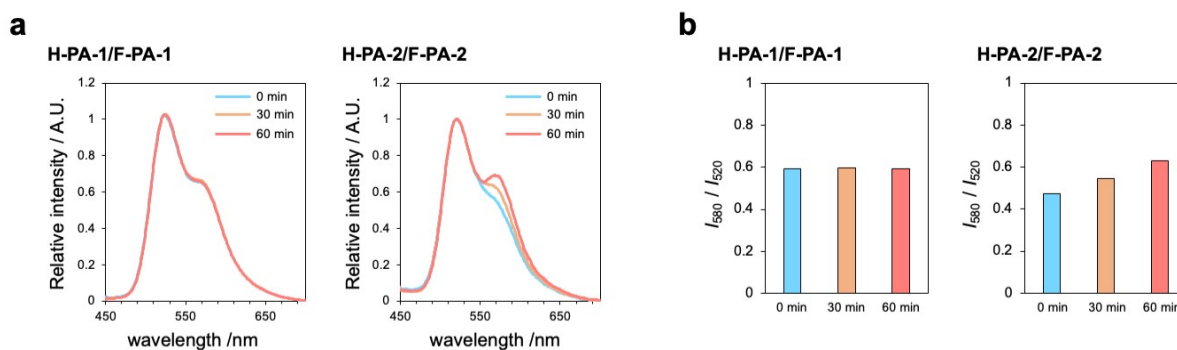


**Fig. S10** (a) Fluorescence spectra of mixtures of H-PA-1/F-PA-1 and H-PA-2/F-PA-2 (H-PA:F-PA = 1:1 (mol/mol),  $[PA_{total}] = 0.5$  mM in 25 mM MES buffer, pH 7.0) in the presence of 1 mol% FL-H-PA and TMR-F-PA. PA mixtures were incubated at 363 K for 0, 30, or 60 min before cooling to 310 K.  $\lambda_{ex} = 420$  nm and  $T = 298$  K. (b) Ratios of fluorescence intensities at 580 nm from TMR and at 520 nm from FL at various incubation time at 363 K.

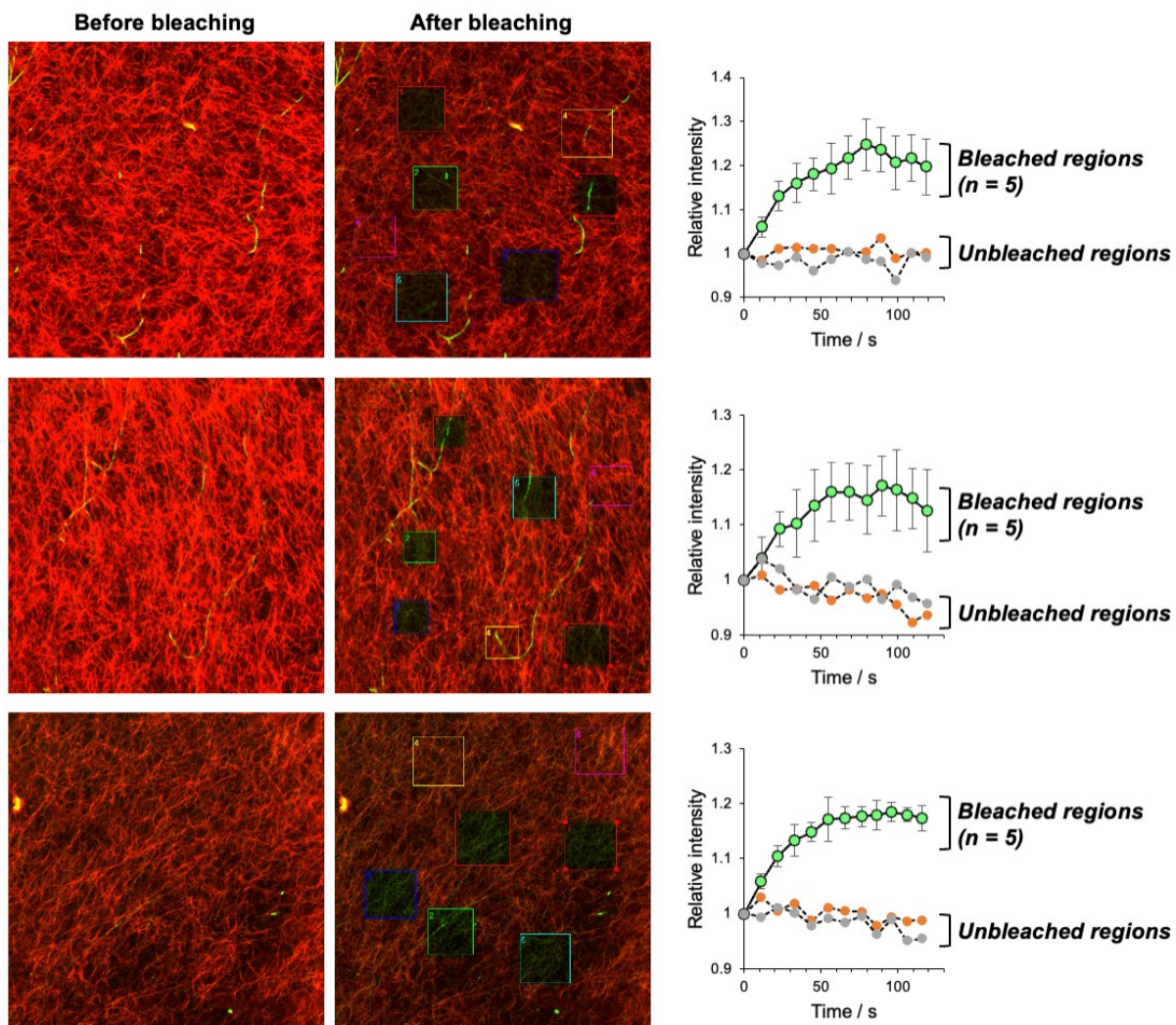


**Fig. S11** Recovery of fluorescence from donor (FL) after bleaching acceptor (TMR) dye in H-PA-2/F-PA-2 assemblies that were incubated 60 min at 363 K before cooling to 310 K. Confocal images of three representative places before bleaching (left) and after bleaching (middle). Changes in relative fluorescence intensities of FL at bleached (5 ROIs in each image) and unbleached regions (2 ROIs in each image) (right).

## 10. Assembly formation with and without incubation at 363 K

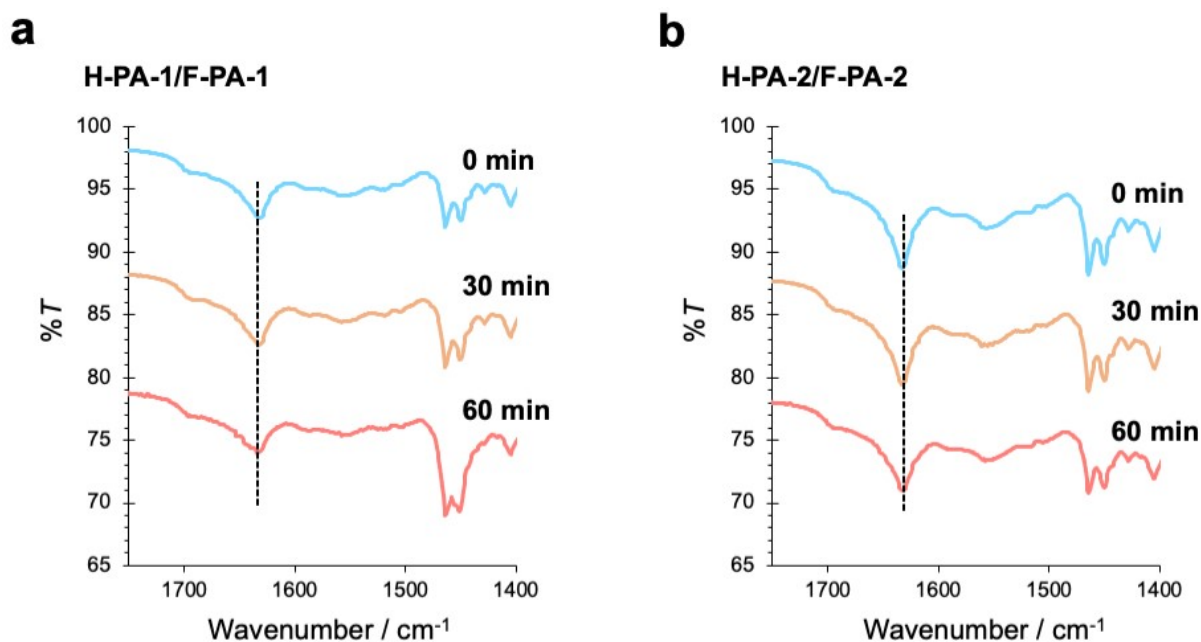


**Fig. S12** FT-IR spectra of mixtures of H-PA-1/F-PA-1 and H-PA-2/F-PA-2 (H-PA:F-PA = 1:1 (mol/mol), [PA<sub>total</sub>] = 0.5 mM in 25 mM MES buffer, pH 7.0) with various incubation times at 363 K before cooling to 310 K. Freeze-dried solids of each sample were used for the measurement in ATR mode.

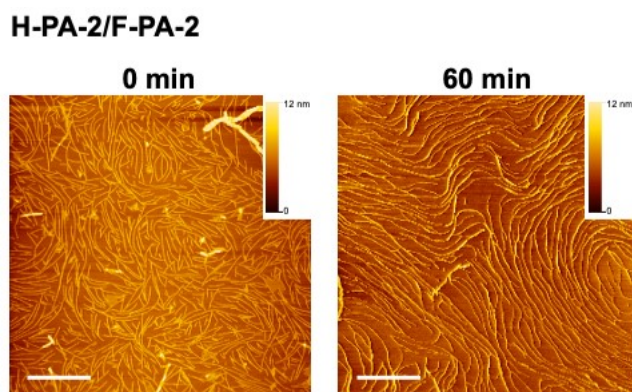


**Fig. S13** SPM images of H-PA-2/F-PA-2 assemblies with 0 or 60 min incubation at 363 K before cooling to 310 K. Samples were placed onto a freshly cleaved mica and images were acquired with a Hitachi Nanocute in the dynamic force mode using a SI-DF3P2 cantilever. Bars: 1 μm.

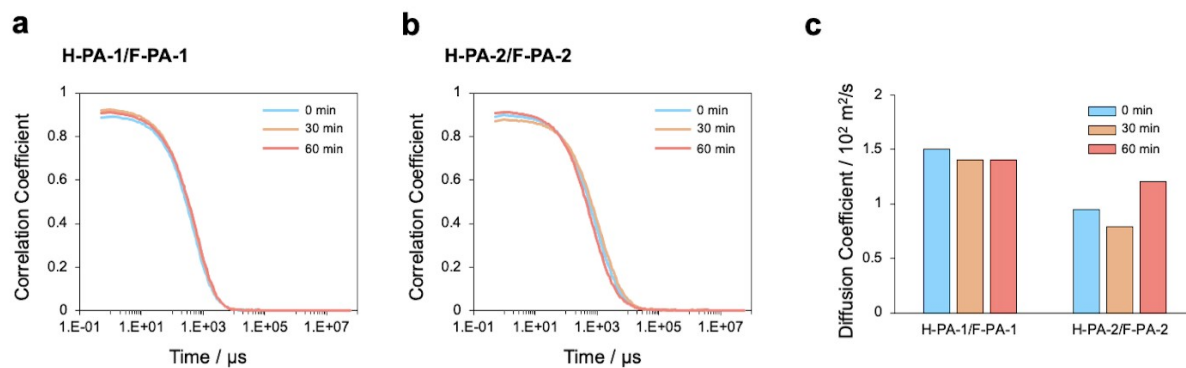


**Fig. S14** (a, b) Correlation coefficients of H-PA-1/F-PA-1 (a) and H-PA-2/F-PA-2 (b) mixtures and (c) diffusion coefficients of the mixtures with incubation at 363 K for 0, 30, or 60 min.

## 11. Dissipative particle dynamics simulation

We use a coarse-grained model for amphiphilic molecules, as shown in Fig. S10. The amphiphilic molecule is represented by a hydrophilic group composed of three particles and a hydrophobic group. To reveal the effect of the length in the hydrophobic part, the number of particles in the hydrophobic group is varied from three to five.

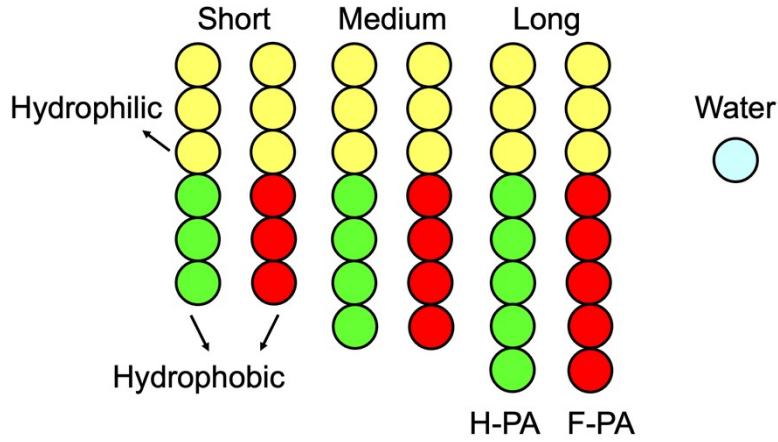


**Fig. S15** Coarse-grained models for amphiphilic molecules consisting of hydrophilic and hydrophobic parts. Three different lengths of the hydrophobic part are prepared. Yellow spheres represent hydrophilic particles. Green and red and green spheres represent hydrophobic alkyl and fluoroalkyl tails, respectively.

We use the dissipative particle dynamics (DPD) method.<sup>S1</sup> In the DPD method, the motion of the particles is given by Newton's equation with a pairwise Langevin thermostat.

$$\frac{d\mathbf{r}_i}{dt} = \mathbf{v}_i, \quad m \frac{d\mathbf{v}_i}{dt} = \sum_{i \neq j} (\mathbf{F}_{ij}^C + \mathbf{F}_{ij}^D + \mathbf{F}_{ij}^R).$$

The conservative force is calculated as  $\mathbf{F}_{ij}^C = a_{ij} \omega(r_{ij}) \Theta(1 - r_{ij} / \sigma) \hat{\mathbf{r}}_{ij}$ , where  $a_{ij}$  is the maximum repulsive force strength,  $\omega(r_{ij}) = 1 - r_{ij} / \sigma$ ,  $\sigma$  is the cut-off length,  $\mathbf{r}_{ij} = \mathbf{r}_i - \mathbf{r}_j$ ,  $r_{ij} = |\mathbf{r}_{ij}|$ ,  $\hat{\mathbf{r}}_{ij} = \mathbf{r}_{ij} / r_{ij}$ , and  $\Theta$  is the unit step function. The dissipation force is calculated as  $\mathbf{F}_{ij}^D = -\gamma_{ij} \omega^2(r_{ij}) (\hat{\mathbf{r}}_{ij} \cdot \mathbf{v}_{ij}) \Theta(1 - r_{ij}) \hat{\mathbf{r}}_{ij}$ , where  $\mathbf{v}_{ij} = \mathbf{v}_i - \mathbf{v}_j$ , and  $\gamma_{ij}$  is a friction parameter and set as  $4.5m/\tau$ , where  $\tau = \sigma \sqrt{m / k_B T}$  is the unit time in the simulation. The random force is calculated as  $\mathbf{F}_{ij}^R = \sigma_{ij} \omega(r_{ij}) \xi_{ij} \Theta(1 - r_{ij}) \hat{\mathbf{r}}_{ij}$ , where  $\sigma_{ij}$  is noise strength.



The Gaussian white noise  $\xi_{ij}$  satisfies the fluctuation and dissipation theorem:  $\langle \xi_{ij}(t) \rangle = 0$  and  $\sigma_{ij}^2 \langle \xi_{ij}(t) \xi_{kl}(t') \rangle = 2\gamma_{ij} k_B T (\delta_{ik} \delta_{jl} + \delta_{il} \delta_{jk}) \delta(t-t')$ , where  $k_B T$  is the thermal energy. The bond force connects particles in molecules in Fig. SX-1:  $\mathbf{F}_{ij}^B = C(1 - r_{ij}/r_b) \mathbf{r}_{ij}$ , where  $C = 40k_B T / \sigma$  is the bond strength and  $r_b = 0.50\sigma$  is the bond length.

We use the  $a_{ij}$  parameters summarized in Supplementary Table S1. The hydrophobicity of tail particles,  $a_{HB}$ , varies from 55 to 90.

**Supplementary Table S1.** Repulsive interaction parameters  $a_{ij}$  with units  $k_B T$ .

	W	H	T (alkyl)	T
W	25	25	$a_{HB}$	$a_{HB}$
H		25	$a_{HB}$	$a_{HB}$
T (alkyl)			25	50
T				25

DPD simulations are performed using the LAMMPS program.<sup>S2</sup> All simulations are carried out in an  $NVT$  ensemble (constant number  $N$  of particles, volume  $V$ , and temperature  $T$ ) at the particle density  $N/V = 3$ . The cubic simulation boxes  $L_x = L_y = L_z = 50\sigma$  are used. The numbers of molecules for short, medium, and long tails are 2380, 2040, and 1785, respectively, where the ratio of particles in the amphiphilic molecules is 7.616% in the simulation system. The integration time step is set as  $\Delta t = 0.02\tau$ . To prepare the randomly mixed state for the initial condition, the simulation is performed with all  $a_{ij} = 25$  for  $2 \times 10^3 \tau$ .

To reveal the degree of the phase separation between molecules with alkyl and fluoroalkyl tails, we calculate the ratio of the surrounding hydrophobic particle types,  $\phi$ , where the number of particles of the same type in the surroundings is divided by the number of all hydrophobic particles in the surroundings. The cut-off length to count the surroundings is the same as  $\sigma$ .

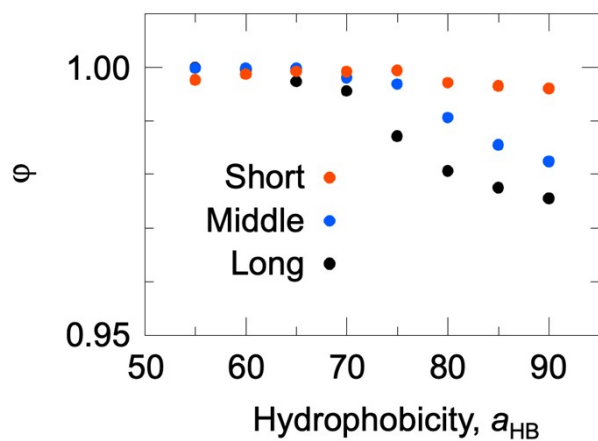


**Fig. S16** The degree of the phase separation,  $\phi$ , between molecules with alkyl and fluoroalkyl tails. The numbers are averaged during the  $10^4$ – $2 \times 10^4$  simulation time. We confirm the repeatability by calculating four different initial conditions. An influence of the integration time step is also checked with  $\Delta t = 0.01\tau$ .

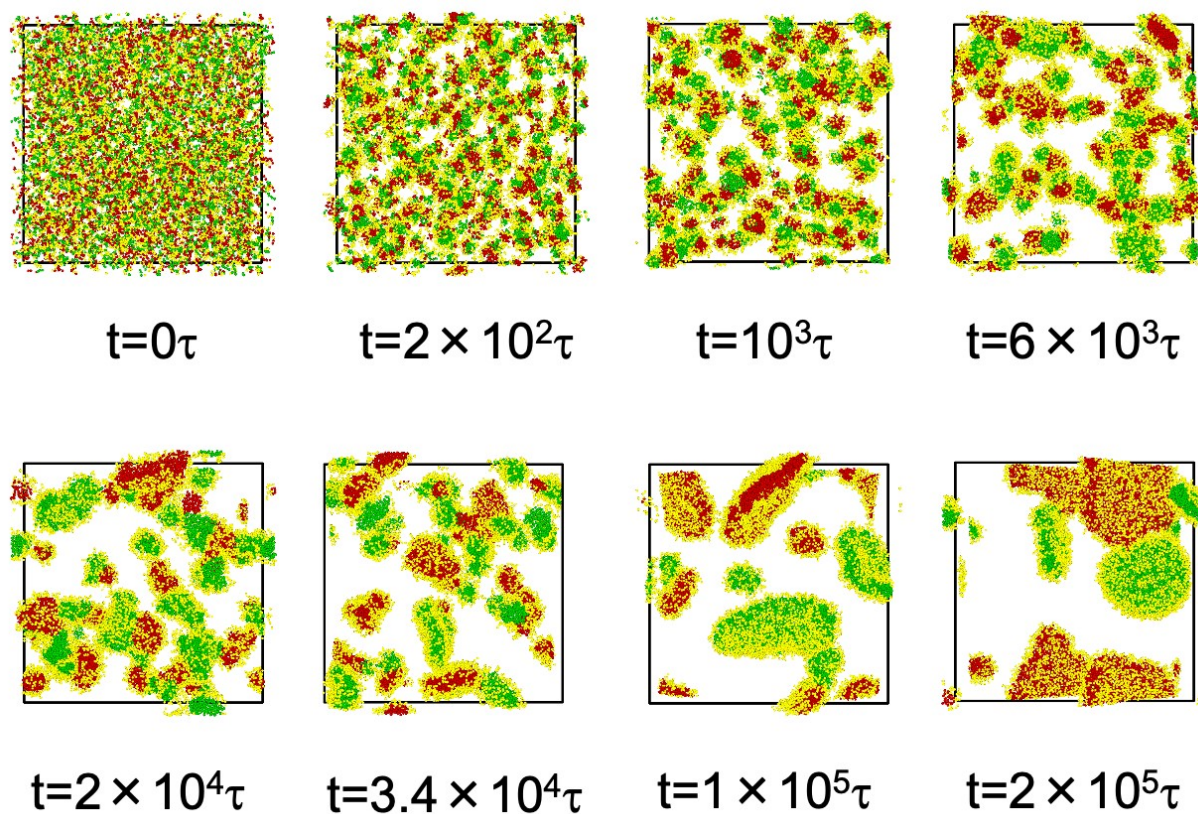


**Fig. S17** Simulation snapshots of amphiphilic molecules with the medium tail at high hydrophobicity ( $a_{\text{HB}}=85$ ). Water particles are displayed transparently.

## References

- [S1] Groot, R. D. & Warren, P. B. Dissipative particle dynamics: Bridging the gap between atomistic and mesoscopic simulation. *J. Chem. Phys.* **107**, 4423–4435 (1997).
- [S2] Plimpton, S. Fast Parallel Algorithms for Short-Range Molecular Dynamics. *J. Comput. Phys.* **117**, 1–19 (1995).